HHLA2 promotes tumor progression by long non-coding RNA H19 in human gallbladder cancer

YIZHOU ZHANG[1], HANRONG LI[2], CHAO LV[1], BAOKANG WU[1], YANG YU[3], CHONGLI ZHONG[1], QI LANG[1], ZHIYUN LIANG[1], YANG LI[1], YU SHI[1], JIAN ZHANG[4], FENG XU[1] and YU TIAN[1]

[1]Department of General Surgery, Shengjing Hospital of China Medical University, Shenyang, Liaoning 110004; [2]Department of Ophthalmology, Fourth Affiliated Hospital of China Medical University, Shenyang, Liaoning 110005; [3]Department of Surgery, Jinzhou Medical University, Jinzhou, Liaoning 121001; [4]Department of Oncology, Liaoyang Central Hospital of China Medical University, Liaoyang, Liaoning 111010, P.R. China

Received March 22, 2022; Accepted June 16, 2022

DOI: 10.3892/ijo.2022.5402

Abstract. Advanced gallbladder cancer (GBC) is one of the most malignant of all types of biliary tract cancers that is associated with poor prognosis and high mortality. Accumulating evidence suggest that the B7 family of proteins serve an essential role in various types of cancers, including GBC. However, the potential function and regulatory mechanism of human endogenous retrovirus-H long terminal repeat-associating protein 2 (HHLA2; also known as B7-H7 or B7H5) in GBC remain poorly understood. In the present study, immunohistochemistry was used to examine the expression pattern of HHLA2 in samples from 89 patients with GBC. The possible association between HHLA2 expression and the clinicopathological parameters, including prognosis, were then assessed. Using lentiviruses, overexpression of HHLA2 plasmid or short-hairpin RNA (shRNA) of HHLA2 were transfected into GBC-SD cells to overexpress or knock down HHLA2 expression, respectively. The effects of HHLA2 overexpression and knockdown on the epithelial-mesenchymal transition (EMT) process on GBC-SD cells were measured by the western blotting and immunofluorescence staining of collagen I, N-cadherin, E-cadherin, vimentin and α-SMA. By contrast, changes in cell proliferation were measured using EdU assay. Cell invasion and migration were assessed using Transwell and wound-healing assays, respectively. In addition, a xenograft mouse model was established to evaluate the tumorigenic ability of the GBC cell line *in vivo* after stable transfection with lentivirus for HHLA2 overexpression or shRNA for HHLA2 knockdown. The regulatory relationships among TGF-β1, long non-coding RNA (lncRNA) H19 (H19) and HHLA2 were then investigated. The mRNA expression of lncRNA H19 were assessed using reverse transcription-quantitative PCR, whereas the expression levels of HHLA2 were detected by western blotting and immunofluorescence staining. HHLA2 expression was found to gradually increase as the stages of the GBC samples become more advanced. In addition, the expression level of HHLA2 was calculated to be positively associated with the Nevin stage, American Joint Committee on Cancer stage, tumor invasion and regional lymph node metastasis but was negatively associated with the overall patient survival (OS). *In vitro* experiments demonstrated that overexpression of HHLA2 promoted GBC migration, invasion, proliferation and EMT, whereas *in vivo* experiments found a promoting role of HHLA2 overexpression on GBC tumor growth. After transfection with lentiviruses encoding the overexpression plasmid of lncRNA H19, GBC migration, invasion, proliferation and EMT were increased. By contrast, knocking down HHLA2 expression suppressed TGF-β1- or lncRNA H19 overexpression-induced GBC migration, invasion, proliferation and EMT. In addition, HHLA2 knockdown significantly reduced the sizes of the GBC tumors *in vivo*. These results suggest that HHLA2 overexpression can promote GBC progression. Conversely, ablation of HHLA2 expression inhibited both TGF-β1- and lncRNA H19-induced GBC progression, suggesting that HHLA2 is a potential therapeutic target for this disease.

Correspondence to: Professor Yu Tian, Department of General Surgery, Shengjing Hospital of China Medical University, 36 Sanhao Street, Shenyang, Liaoning 110004, P.R. China
E-mail: yu.tian@cmu.edu.cn

Key words: human endogenous retrovirus-H long terminal repeat-associating protein 2, target therapy, gallbladder cancer, epithelial-mesenchymal transition, TGF-β1, long non-coding RNA H19

Introduction

Gallbladder cancer (GBC) is the one of the highest incidence and a particularly aggressive biliary tract cancer (1). Epidemiologically, it tends to be more commonly found in women, with high rates of recurrence and mortality, which is reflected by it having the worst overall survival (OS) rate among all other biliary tract cancer types (2-6). In 2018, ~219,420 new cases and 165,087 cases of mortality due to GBC were reported globally (7). Although surgical treatment is currently the most effective method for treating GBC, the majority of patients with GBC are typically already at metastatic or late

clinical stages at diagnosis on presentation, limiting the curative treatment options (8-10). Therefore, it remains in high demand to develop novel precise targeted treatment methods to inhibit the progression of GBC whilst also improving the prognosis of treatment strategies. The diverse characteristics of GBC pathogenesis leads to poor prognoses according to a previous gene set enrichment analysis, specifically due to epithelial-mesenchymal transition (EMT), angiogenic immune suppression and hypoxia (11). According to a previous Kyoto Encyclopedia of Genes and Genomes analysis, overactivation of the TGF-β pathway in GBC can lead to significantly poorer survival outcomes (11,12). However, the detailed mechanism underlying EMT and the TGF-β pathway in GBC require further study.

Members of the B7/CD28 family have been previously found to regulate the immune response and cancer invasion, in both positive and negative manners (13). Human endogenous retrovirus-H long terminal repeat-associating protein 2 (HHLA2; also known as B7H7 or B7H5) is the only member of the B7 protein family found in humans (14). HHLA2 cannot be found in mice and is mainly expressed in human breast, lung, thyroid, melanoma, pancreas, ovary, liver, bladder, colon, prostate, kidney and esophagus cancer cells, activated myeloid cells, monocyte-derived macrophages and dendritic cells (14). Previous studies have found that HHLA2 can activate antigen-presenting cells in response to inflammation (14,15). In addition, HHLA2 interacts with the co-receptor CD28H to stimulate T cell proliferation, differentiation and the production of cytokines, including IFN-γ, IL-2 and IL-10 (14,15). However, HHLA2 can also bind to another inhibitory receptor, three immunoglobulin domains and long cytoplasmic tail 3 (KIR3DL3), which inhibits T cell action (16). In terms of cancer, higher expression levels of HHLA2 were previously reported to be associated with poorer prognoses or higher degrees of tumour invasion in lung carcinoma, hepatocellular carcinoma and prostate cancer (17-19). By contrast, in epithelial ovarian cancer, higher HHLA2 expression levels were demonstrated to be associated with superior survival outcomes and reduced tumor growth (20). Therefore, HHLA2 can serve opposite physiological roles in cancer depending on the malignancy of interest. However, the expression profile of HHLA2 and its relationship with GBC progression remain unclear.

Long noncoding RNAs (lncRNAs) are non-coding transcripts that are >200 bp in length and server important roles in regulating cellular protein expression and function (21). LncRNAs have also been previously found regulate the progression of various cancers. LncRNA H19 (H19) is one such lncRNA, which was one of the earliest discovered lncRNAs (22,23). H19 has been observed to serve a significant role in EMT progression in colorectal cancer, breast cancer and gallbladder cancer (22,23). Furthermore, previous studies have reported that H19 can function as a molecular sponge to restrain the functions of miR-342-3p and promote EMT in GBC (24,25). In the present study, the role of H19-induced upregulation on HHLA2 expression in the molecular regulatory network underlying EMT in GBC was investigated.

Additionally, in the present study, the aim was to investigate the role of HHLA2 in GBC progression and to further evaluate the potential of HHLA2 as a potentially novel therapeutic target.

Materials and methods

Patients and specimens. GBC specimens were collected from patients at Shengjing Hospital of China Medical University (Shenyang, China) from October 20, 2011 to December 10, 2020. Patients diagnosed with GBC and confirmed by pathologists according to the American Joint Committee on Cancer (AJCC) cancer staging system (8th edition) (26) and the 2019 (5th edition) WHO classification of tumours of the digestive system (27), who underwent surgery as the primary treatment and with comprehensive clinical and follow-up data, were included. Patients with preoperative chemotherapy, other concurrent malignant tumors, unsuccessful follow-up or those whose survival data cannot be obtained were excluded from this study. A total of 89 patients were selected from our patient database. Among these patients, 37 were males (42%) and 52 were females (58%). The mean age was 62.34±10.19 years, ranging from 30 to 89 years. This research arm of the present study was approved by the Ethics Committee of Shengjing Hospital of China Medical University (approval no. 2019PS036K). Written consent was obtained from all the patients involved in the present study. Each patient's age, sex, differentiation, Nevin stage (28), tumor invasion, regional lymph node metastasis, distant metastasis and histological stage were obtained.

Follow-up arrangement. The final date of the last follow-up was November 1, 2021. OS was defined as the interval either between the initial diagnosis and mortality or between the initial diagnosis and the date of the last observation for the surviving patients. Data were censored at the date of the last follow-up for any living patients.

Immunohistochemical staining and evaluation. HHLA2 expression in the GBC specimens was measured by immunohistochemistry. The GBC specimens were fixed in a 10% formalin solution for 24 h at room temperature, before they were embedded in paraffin, sliced into 4 μm-thick sections and placed onto glass slides. They were then dehydrated in an ascending ethanol gradient and cleared with xylene. The slices were treated with 95˚C Sodium Citrate Antigen Retrieval Solution (cat. no. C1031; Beijing Solarbio Science & Technology Co., Ltd.) for 10 min. The slices were then treated with 3% H_2O_2 at 37˚C for 10 min and blocked in 3% BSA (Beyotime Institute of Biotechnology) solution for 30 min at room temperature. Immunohistochemical staining were subsequently performed. Rabbit anti-HHLA2 monoclonal antibodies (1:100, cat. no. ab214327; Abcam) were used as the primary antibody and incubated at 4˚C for 10 h, whereas HRP-conjugated goat anti-rabbit IgG was used as the secondary antibody (1:100, cat. no. ab288151; Abcam) and incubated at room temperature for 30 min. Diaminobenzidine (cat. no. DA1010; Beijing Solarbio Science & Technology Co., Ltd.) incubating for 5 min at room temperature was used to develop color reaction. Paraffin sections were counterstained with Haematoxylin (Beijing Solarbio Science & Technology Co., Ltd.) lasting for 2 min at room temperature.

Immunohistochemical staining results were assessed by two different pathologists using light microscopy (magnifications, x200 and x400; Olympus Corporation). In cases where

there was disagreement, the results were evaluated again. If a consensus could not be reached, another pathologist participated in the evaluation. All pathologists were blinded to the patient's clinical data. In summary, ≥ two pathologists must agree with each result. Immunostaining in the tumor tissues was semi-quantified using the ImageJ software (version 1.52; National Institutes of Health), for the staining intensity. The staining intensity was divided into four levels as follows: i) Negative, 0; ii) low positive, 1; iii) positive, 2; and iv) high positive, 3. In total, five high-power fields (magnification, x400) of each slice were randomly selected to judge the corresponding percentage of positive cells. The H-score of each case was measured by multiplying the staining intensity by the corresponding percentage of positive cells (range from 0 to 168). To associate the relationship between HHLA2 and patient outcome, the existence of tumor classifications should be revealed. Since H-score was determined to be continuous variables, the optimal cut-off value was determined using X-tile software (version 3.6.1; https://medicine.yale.edu/lab/rimm/research/software/) to divide the specimens into HHLA2-high group and the HHLA2-low group. The X-tile program performed a single, global assessment of every possible method of dividing the population. In the assessment, each H-score value of all the specimens was used as a cut-off value to divide the specimens into two groups. Subsequently, every χ^2 value of each grouping grouped by different H-score values were calculated using the Kaplan-Meier method respectively to find the highest χ^2 value, which was 7.16 (ranging from 0.40 to 7.16). The grouping with a χ^2 value of 7.16 was regarded as the optimal grouping, where the cut-off value of the optimal grouping was determined as the optimal cut-off value, which was 80 (29). Therefore, specimens with H-score >80 were included in the HHLA2-high group and specimens with H-score ≤80 specimens were included in the HHLA2-low group.

Cell culture. The GBC cell line GBC-SD (cat. no. CSTR:19375.09.3101HUMTCHu16) was purchased from The Cell Bank of Type Culture Collection of the Chinese Academy of Sciences. The cells were cultured in RPMI1640 medium (Gibco; Thermo Fisher Scientific, Inc.) supplemented with 10% FBS (Gibco; Thermo Fisher Scientific, Inc.) and were treated with or without TGF-β1 (PeproTech, Inc). The TGF-β1 cytokine was dissolved in PBS containing 5% Trehalose as storage solution at a concentration of 20 μg/ml. The storage solution of TGF-β1 was added into the culture medium to reach a concentration of 10 ng/ml for treatment for 48 h at 37˚C, whilst the control group received the same amount of vehicle treatment (PBS containing 5% Trehalose). For culturing, 5% CO_2 and 37˚C was applied for the cell lines.

Western blotting. The cells were lysed with RIPA buffer (Beyotime Institute of Biotechnology) for 2 h on ice with a protein inhibitor cocktail (Beyotime Institute of Biotechnology). This mixture was then centrifuged at 12,000 x g for 30 min at 4˚C, before the supernatant was collected and the protein concentration was measured using a BCA kit (Beyotime Institute of Biotechnology). In total, 5X loading buffer was added to the protein solution at a 1:4 ratio and heated at 95˚C for 5 min. After SDS-PAGE in 5% stacking gel and in 10% separating gel (15 μg protein per lane) and transfer onto polyvinyl difluoride membranes (Thermo Fisher Scientific, Inc.), before blocked with 5% skimmed milk powder solution (diluted in Tris-buffered saline containing 0.1% Tween-20) for 2 h under room temperature. After blocking, the membranes were incubated with the corresponding primary antibodies against GAPDH (1:1,000; cat. no. ab181602; Abcam), vimentin (1:1,000; Abcam; cat. no. ab92547), α-smooth muscle actin (SMA; 1:1,000; Abcam; cat. no. ab124964), HHLA2 (1:1,000; Abcam; cat. no. ab214327), E-cadherin (1:1,000; Abcam; cat. no. ab40772), N-cadherin (1:1,000; Abcam; cat. no. ab18203) and Collagen I (Col-I; 1:1,000; Abcam; cat. no. ab34710) for 10 h at 4 ˚C. After incubating with the primary antibodies, the membranes were incubated with HRP-conjugated goat anti-rabbit IgG secondary antibodies (1:5,000; cat. no. ab6721; Abcam) for 1 h at room temperature. Protein expression levels were detected by Chemistar™ High-sig ECL Western Blotting substrate (cat. no. 180-5001; Tanon Science and Technology Co., Ltd.). The western blotting results were quantified using the ImageJ software (version 1.52; National Institutes of Health).

RNA extraction and reverse transcription-quantitative PCR (RT-qPCR). Total RNA was isolated using RNAiso Plus (Takara Bio, Inc.) according to the manufacturer's protocol and reverse transcribed into cDNA using the PrimeScript™ RT Master Mix kit (Takara Bio, Inc.). The temperature protocol was 37˚C for 15 min, 85˚C for 5 sec and 4˚C for 1 h. qPCR was performed using the TB Green™ Premix Ex Taq™ II (Takara Bio, Inc.) and a Roche 96 instrument (Roche Diagnostics) to measure mRNA expression. The thermocycling conditions were as follows: Initial denaturation at 95˚C for 30 sec; followed by 40 cycles at 95˚C for 5 sec and 60˚C for 30 sec; Relative mRNA expression levels were determined using the $2^{-\Delta\Delta Cq}$ method (30), where the experiments were repeated three times. GAPDH was used as the internal control. The GAPDH primers were purchased from Guangzhou RiboBio Co., Ltd. The sequences for GAPDH primers were: Forward, 5'-GAACGGGAAGCTCACTGG-3', and reverse, 5'-GCCTGCTTCACCACCTTCT-3', The sequences of the H19 primers were H19-forward, 5'-CGTGACAAGCAGGACATGACA-3' and reverse, 5'-CCATAGTGTGCCGACTCCG-3'.

Immunofluorescence staining. Cultured cells were first fixed in 4% paraformaldehyde at room temperature for 30 min, before they were blocked with 5% BSA (Beyotime Institute of Biotechnology) at room temperature for 1 h and permeabilized with 0.1% Triton X-100 at room temperature for 15 min. Next, the cells were incubated with 1:200 diluted primary antibodies against vimentin (cat. no. ab92547; Abcam), α-smooth muscle actin (cat. no. ab124964; Abcam), HHLA2 (cat. no. ab214327; Abcam), E-cadherin (cat. no. ab40772; Abcam), N-cadherin (cat. no. ab18203; Abcam) and Col-I (cat. no. ab34710; Abcam) for 10 h at 4˚C. After washing three times with PBS containing 0.1% Tween-20 (PBST), the cells were incubated in 1:200 diluted Goat anti-Rabbit IgG (H+L) Highly Crossed-Adsorbed Secondary Antibody, Alexa Fluor™ 488 (cat. no. A-11034; Thermo Fisher Scientific, Inc.) for 1 h at room temperature, protected from light. DAPI (Thermo Fisher Scientific, Inc.) at the concentration of 300 nM was used to stain nuclei for 5 min

at room temperature. Protein expression was observed and recorded by fluorescence microscopy (magnification, x200; Olympus Corporation).

Construction of stably transfected cell lines. Lentiviruses encoding the short hairpin (sh)RNA silencing HHLA2 and non-target shRNA, the HHLA2 (GenBank accession no. NM_007072) or H19 (GenBank accession no. NR_ (NR_002196) overexpression vector and empty control lentiviral vector were designed and synthesized by Shanghai GeneChem Co., Ltd. The overexpression vector was sent for sequencing and designated GV348 [Ubi-MCS-SV40-Puromycin]. The knockdown vector was sent for sequencing and designated GV112 [hU6-MCS-CMV-Puromycin]. In brief, the 20 μg GV348 vectors were co-transfected with 15 μg pHelper 1.0 (envelope plasmid) and 10 μg pHelper 2.0 (packaging plasmid) in the 2nd generation transfection system into 293T cells (The Cell Bank of Type Culture Collection of the Chinese Academy of Sciences) cultured in DMEM (Hyclone; Cytiva) with 10% FBS (Hyclone; Cytiva) at 37˚C with 5% CO_2. After 48 h culturing at 37˚C, the supernatant of the 293T cells were collected and the lentivirus was concentrated through centrifugation of 25,000 g at 4˚C for 2 h. Subsequently, the GBC-SD cell lines were plated into six-well plates until reaching 80% confluence, before the lentivirus was added and co-cultured with the cells for 24 h at 37˚C (multiplicity of infection, 10). The medium was then replaced prior to another 48 h of incubation in the 5% CO_2 and 37˚C incubator. Subsequently, 25 μg/ml puromycin treatment for 2 weeks at 37˚C was used to select for the stably transfected cell lines before the knockdown efficiency was confirmed by western blotting or RT-qPCR after the cell line reached a confluence of 80%. In the rescue experiments, HHLA2-shRNA or NC-shRNA was transfected into H19-overexpressing GBC-SD cells. In total, 24 h after transfection, the cells were harvested for subsequent experiments. The target sequence of shRNA for HHLA2 was 5'-ATCCCGATTCTCATGGAACAA-3', whereas the target sequence of NC shRNA was 5'-TTCTCC GAACGTGTCACGT-3'.

Wound healing assay. The GBC-SD cells were seeded into six-well plates, and cultured until 100% confluence. A 20-μl sterile yellow plastic pipette tip was then used to scratch the cell monolayer. After 48 h of incubation with or without 10 ng/ml TGF-β1 at 37˚C with serum-free RPMI1640 medium, the scratches were imaged by light microscopy (magnification, x200) and analysed by ImageJ software (version 1.52; National Institutes of Health). Migration area was calculated by multiplying the migration distance (scratch width observed at 0 h-scratch width observed at 48 h) with the width of field of view (500 μm). Relative migration area was calculated by dividing the migration area by the migration area of each control group.

Transwell assay. Transwell (Corning, Inc.) chambers were fist pre-coated at 37˚C for 30 min with Matrigel (cat. no. 356234; BD Biosciences) that was diluted at 1:8 with serum-free RPMI1640 medium. In total of $2x10^4$ GBC-SD cells suspended with serum-free RPMI-1640 medium with or without 10 ng/ml TGF-β1 were seeded into the upper surfaces of each Transwell chambers, whilst the lower chambers were added with RPMI-1640 medium with 10% FBS. while the lower chambers were filled with culture medium with 10% FBS. After 48 h invasion at 37˚C, the cells that had not passed through the chamber membrane were gently removed with a wet cotton ball. The membranes were then fixed with 4% paraformaldehyde at room temperature for 30 min and stained with 0.1% crystal violet at room temperature for 15 min and photographed under a light microscope (magnification, x200). In total, five high-power fields (magnification, x200) of each membrane were randomly selected for calculating the cell numbers by ImageJ software (version 1.52; National Institutes of Health).

EdU assay. An EdU assay was performed to evaluate the proliferation levels of the cells using Cell-Light Edu Apollo 488 *In Vitro* Kit (cat. no. C10310-3; Guangzhou RiboBio Co., Ltd.). Briefly, GBC-SD cells were labelled with 50 μM EdU (100 μl/well) for 2 h in a 5% CO_2 and 37˚C incubator. After fixation with 4% paraformaldehyde at room temperature for 30 min, the cells were permeabilized with 0.5% Triton X-100 at room temperature for 10 min. Next, the cells were incubated with 1X Apollo staining solution of the EdU kit at room temperature for 30 min before the nuclei were stained with DAPI (Thermo Fisher Scientific, Inc.) at the concentration of 300 nM for 5 min at room temperature. The cells were observed and imaged by fluorescence microscopy (magnification, x200).

Xenograft mouse model. The mouse xenograft experimental protocol was approved by the Ethics Committee of Shengjing Hospital of China Medical University (approval no. 2019PS325K) and performed in accordance with the Laboratory Animal Guideline for Ethical Review of Animal Welfare (31). All mice were housed in an animal room at a constant temperature of 25˚C with 30-40% humidity, under a 12-h light/dark cycle and had free access to food and water.

A total of 24 6-week-old female BALB/c nude mice (weight, 19-22 g) were used to establish the GBC xenograft models. The mice were randomly divided into the HHLA2 overexpression group, NC overexpression group, HHLA2-shRNA group and NC-shRNA group, with 6 mice in each group. After the cells in each group reached a confluence of 80-90%, they were digested with 0.25% trypsin. Next, the cells were resuspended in PBS to form a cellular suspension at a density of $1x10^6$ cells in 100 μl. Under isoflurane inhalation anaesthesia (1-2%), each mouse was gradually and slowly inoculated subcutaneously with 100 μl this cell suspension in the right armpit. The health and behaviour of the mice were monitored once a day to determine if there were difficulties eating or drinking, symptoms of pain or long-term problems without recovery. If the tumor volume was found to be >2,000 mm^3, the animal would be euthanized as a humane endpoint. In total, 18 days after inoculation, all mice were sacrificed by cervical dislocation after isoflurane inhalation (5% for 5 min). Cardiac arrest was then used to verify death by pulse palpation. Tumor tissues were collected for measurement and analysis of the volume and weight. The maximum tumor volume observed was 1,680 mm^3 and the maximum tumour diameter was 15 mm.

Table I. Relationship between HHLA2 expression and clinical characteristics in patients with gall bladder cancer (N=89).

Parameter	Total	HHLA2 expression		P-value
		Low	High	
Patients (n)	89	44	45	
Sex				0.244
Male	37	21	16	
Female	52	23	29	
Age (years)				0.899
<62	49	24	25	
≥62	40	20	20	
Differentiation				0.219
Poorly or moderately	21	13	8	
Well	48	22	26	
Nevin stage				0.014
I-III	37	24	13	
IV-V	52	20	32	
American Joint Committee on Cancer stage				0.007
I-II	36	24	12	
III-IV	53	20	33	
Tumor invasion				
T1-T2	44	27	17	0.026
T3-T4	45	17	28	
Regional node metastasis				
Absent	46	29	17	0.018
Present	31	11	20	
Distant metastasis				
Absent	61	34	27	0.079
Present	28	10	18	

HHLA2, human endogenous retrovirus-H long terminal repeat-associating protein 2.

Statistical analysis. All count data were analysed using the χ^2 test, continuity correction χ^2 test or Fisher's exact test. Survival differences were compared using the Kaplan-Meier method and log-rank test. Multivariate and univariate analyses were performed using a Cox stepwise proportional hazard model. Data for experiments performed in triplicate are expressed as the mean ± standard deviation. Comparisons between two groups were made using the unpaired Student's t-test. Differences among groups were tested using one-way analysis of variance (ANOVA) and Tukey's post hoc test. SPSS software version 26.0 (IBM Corp.) or GraphPad Prism 8.0 (GraphPad Software, Inc.) was used to perform the statistical analysis. $P<0.05$ was considered to indicate a statistically significant difference.

Results

HHLA2 is upregulated in progressed gallbladder cancer, and high expression of HHLA2 is associated with a poor prognosis. The basic clinical characteristics of 89 patients with GBC are summarized in Table I. In total, 37 (42%) of the patients with GBC had a lower Nevin staging of I-III, whereas 58% (n=52) had a high grade (IV-V). According to the AJCC 8th edition cancer staging system, the tumour invasions were classified into two groups, namely the low group (stage I-II; 36 cases; 40%) and the high group (stage III-IV; 53 cases; 60%). Tumour invasions were also classified into two groups, where the low group included T1 and T2 (44 cases; 49%) and the high group included T3 and T4 (45 cases; 51%). In terms of regional lymph node metastasis, 31 (34%) patients had regional lymph node metastasis, whilst 46 (52%) patients did not. For distant metastasis, 28 (31%) patients had distant metastasis (to the liver, intestine and peritoneum), whereas 61 (69%) patients did not. At the end of the follow-up period, 50 patients had succumbed to the disease, where the median follow-up duration was 70 months (range, 1 to 114).

To detect the HHLA2 expression spectrum in the GBC tissues, immunohistochemistry was performed. As shown in Fig. 1A, which shows a cross section of the GBC tissue, HHLA2 was expressed in the membrane and/or cytoplasm in GBC tissues and corresponding adjacent noncancerous

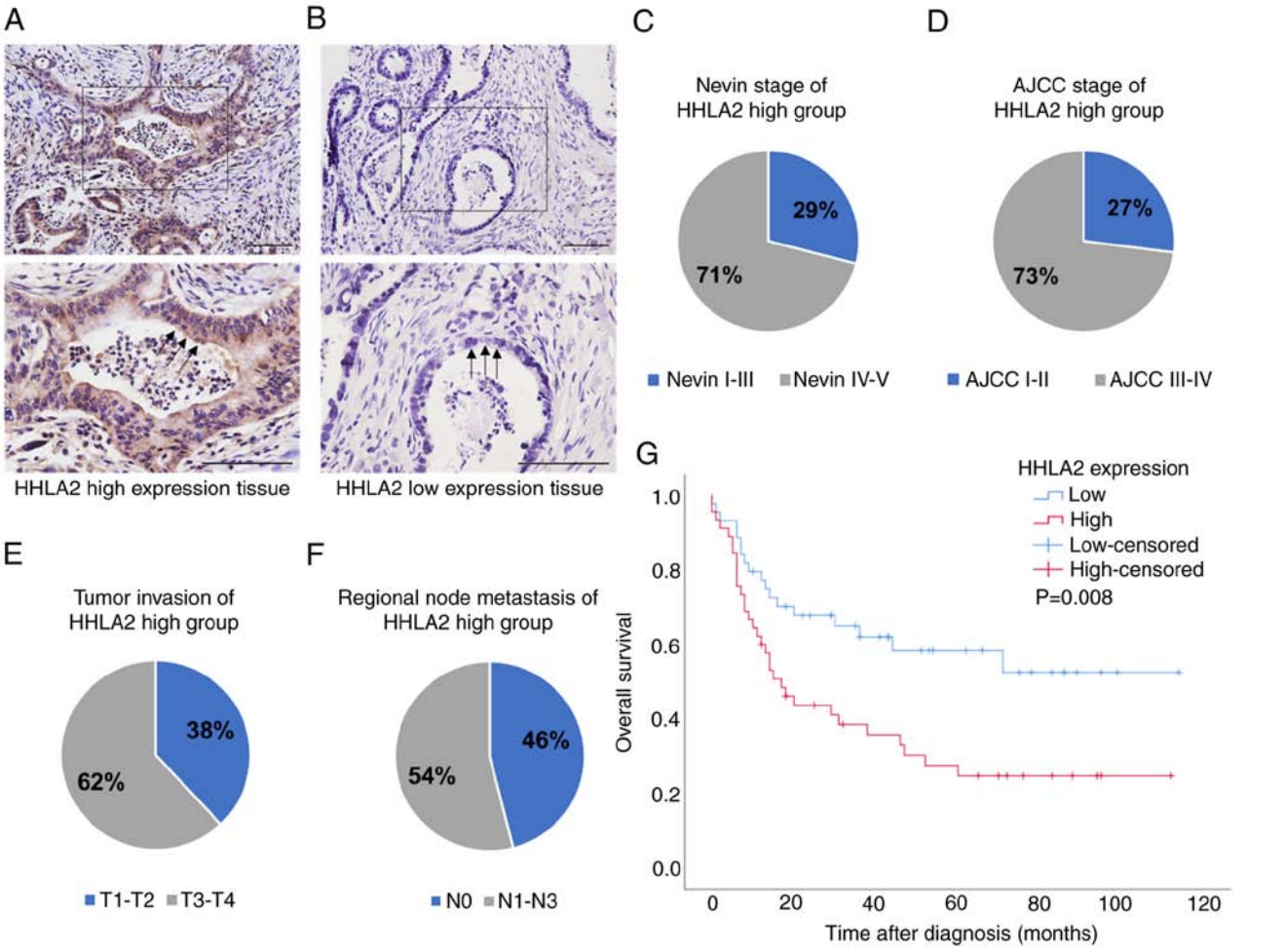

Figure 1. HHLA2 expression is higher in more advanced gall bladder cancer tissues. Immunohistochemical staining of GBC tissues with (A) high HHLA2 expression and (B) low HHLA2 expression. Scale bars, 100 μm. (C) Nevin stage, (D) AJCC stage, (E) tumour invasion and (F) regional node metastasis in the HHLA2-high group. (G) Association of HHLA2 expression with the overall survival according to Kaplan-Meier survival curves. HHLA2, human endogenous retrovirus-H long terminal repeat-associating protein 2; gall bladder cancer; AJCC, American Joint Committee on Cancer.

tissues. The intense staining was predominately seen in apical surfaces of the papillary epithelium and luminal surfaces of the glands (black arrows). Compared with tissues with low HHLA2 expression, HHLA2 high expression tissue showed higher staining intensity and percentage of positively staining cells. Positive HHLA2 staining was observed in all 89 cases (100%). To evaluate the association between HHLA2 expression and various clinicopathological parameters of GBC progression, the cases were subdivided into two groups: HHLA2-high group (45 cases, 51%) and the HHLA2-low group (44 cases, 49%; Fig. 1A and B). HHLA2 expression was found to be positively associated with tumour progression (Fig. 1; Table I). Specifically, 32 cases in the HHLA2-high group reached Nevin stage IV-V, accounting for 71% (Fig. 1C). In addition, 33 cases in the HHLA2-high group reached AJCC stage III-IV, accounting for 73% (Fig. 1D), whilst 28 cases in the HHLA2-high group exhibited tumor invasion T3-T4, accounting for 62% (Fig. 1E). In terms of regional lymph node metastasis, 20 cases in the HHLA2-high group were demonstrated to be positive, accounting for 54% (Fig. 1F). According to Table I, higher HHLA2 expression was significantly associated with Nevin stage, AJCC stage, tumour invasion and regional lymph node metastasis.

Subsequently, univariate analysis of OS was performed to analyse the clinical prognosis of the patients with GBC. The OS of the HHLA2-high group was found to be shorter compared with that in the HHLA2-low group (hazard ratio=2.15; 95% CI=1.20-3.83; P=0.01), where patients with GBC and higher HHLA2 expression tended to have significantly shorter survival times (Fig. 1G).

HHLA2 overexpression promotes EMT in GBC in vitro. To further explore the function of HHLA2 in the GBCs, the GBC-SD cell line were transfected with the HHLA2 plasmid for overexpression. The efficiency of this HHLA2 overexpression in GBC-SD cells was verified by western blot analysis (Fig. 2A and B). Subsequently, the expression of EMT markers α-SMA, vimentin, N-cadherin and Col-I were all significantly increased, whereas the expression of E-cadherin was significantly decreased, in HHLA2-overexpressing GBC-SD cells compared with those in the HHLA2-NC cells (Fig. 2C and D). The relative expression levels of these markers were then observed through immunofluorescence staining, which yielded similar observations compared with those from western blotting. These results suggest that HHLA2 can promote EMT in GBC (Fig. 2E).

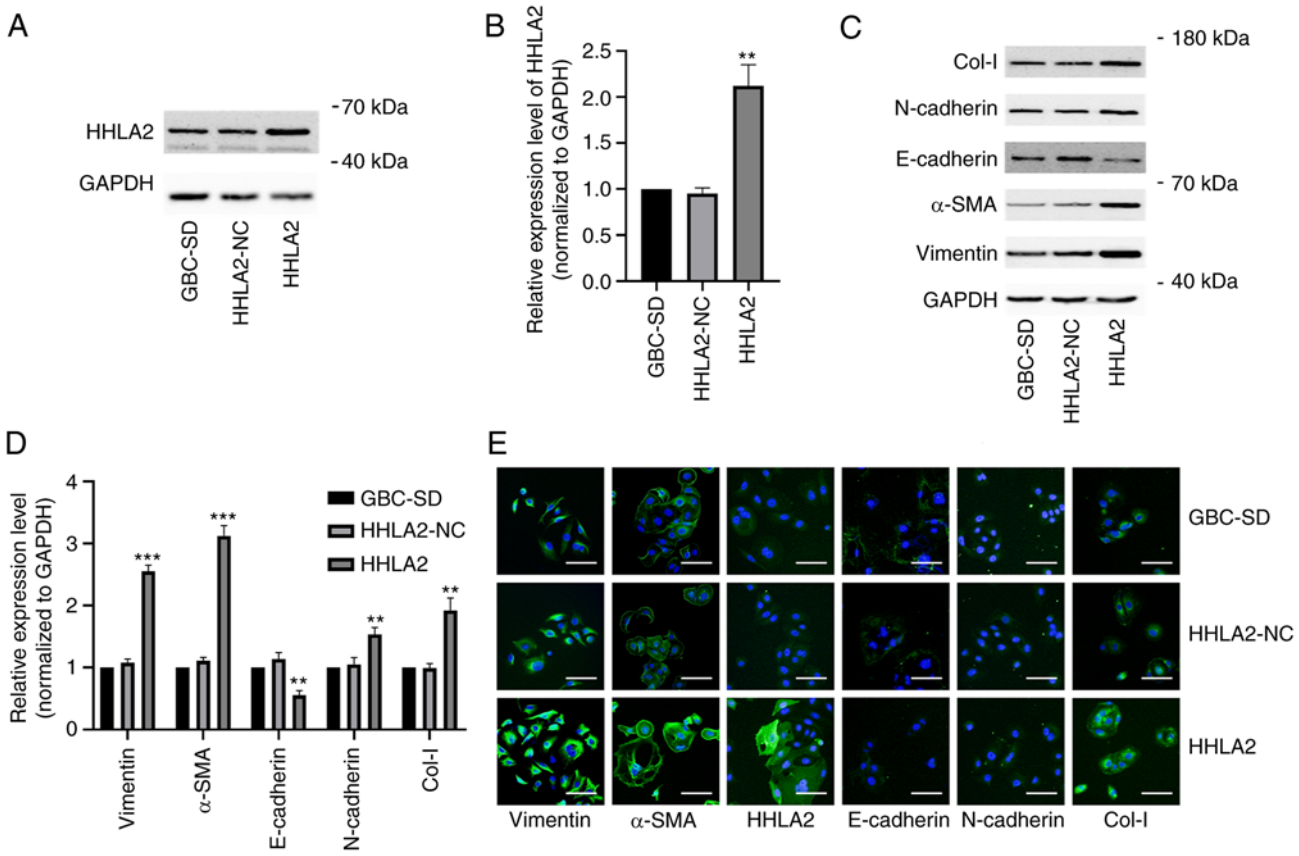

Figure 2. Overexpression of HHLA2 promotes the EMT process in gall bladder cancer cells *in vitro*. (A) Overexpression of HHLA2 was evaluated by western blotting and (B) quantified. (C) Expression of EMT markers Col-I, N-cadherin, α-SMA and vimentin were increased whilst that of E-cadherin was decreased in the HHLA2 overexpression group according to western blotting and (D) subsequent quantification. GAPDH was used as the internal reference protein. The data are expressed as the mean ± SD with n=3. (E) Immunofluorescence staining was utilized to evaluate the expression of EMT markers and HHLA2. Scale bars, 100 μm. Green, target protein; Blue, DAPI. **P<0.01 and ***P<0.001 (HHLA2 group vs. HHLA2-NC group). HHLA2, human endogenous retrovirus-H long terminal repeat-associating protein 2; EMT, epithelial-mesenchymal transition; Col-I, collagen I; α-SMA, α-smooth muscle actin.

HHLA2 exerts oncogenic functions in GBC. Changes in the migratory ability of GBC-SD cells after HHLA2 overexpression was next measured using wound-healing assays. Overexpression of HHLA2 led to significantly more potent migratory capabilities compared with those in the HHLA2-NC group (Fig. 3A and B). The invasive abilities of these HHLA2-overexpressing cells were next explored through Transwell assays. The results demonstrated a significantly higher invasive ability in the HHLA2-overexpressing cell line compared with that in the HHLA2-NC group (Fig. 3C and D). An EdU assay was used to investigate the proliferation of GBC-SD cells, which revealed that there was a significant increase in the proliferation of the HHLA2-overexpressing cell line compared with that in the HHLA2-NC group (Fig. 3E and F). These results suggest that HHLA2 can mediate oncogenic functions in GBC *in vitro*.

To determine whether HHLA2 can regulate the tumorigenic ability of GBC *in vivo*, a xenograft mouse tumor model was established. HHLA2 is not expressed in the mouse genome (14), negating the requirement for measuring the protein or mRNA expression levels in these samples prior to the establishment of this xenograft model. The GBC cell line stably overexpressing HHLA2 and the negative control group were injected into the left flanks of six nude mice in each group. After 18 days, compared with those in the negative control group, tumors in the HHLA2 overexpression group exhibited a significantly larger volume and were heavier in weight (Fig. 3G-I). Taken together, these results suggest that HHLA2 can promote the tumorigenic ability of GBC *in vivo*.

HHLA2 knockdown impedes EMT in GBC. To determine if HHLA2 has the potential to become a therapeutic target in GBC, GBC-SD cells were transfected with HHLA2-shRNA to knock down HHLA2 expression in GBC-SD cells. The knockdown efficiency was validated by western blotting (Fig. 4A and B). According to western blotting and immunofluorescence staining data, HHLA2 knockdown led to significant decreases in the expression of Col- I, N-cadherin, α-SMA and vimentin but significant increases in the expression of E-cadherin in GBC-SD cells (Fig. 4C-E). TGF-β1-induced EMT *in vitro* model was next established (Fig. S1A and B). There was a significant increase in the expression of HHLA2 in the GBC cells (Fig. S1A and B), which was reversed by transfection with HHLA2-shRNA. In addition, transfection with HHLA2-shRNA significantly reduced the expression of the EMT biomarkers compared with that in the TGF + sh-NC group (Fig. S1C-E). These results suggest that downregulation of HHLA2 can inhibit EMT in GBC both alone and/or in the presence of TGF-β1.

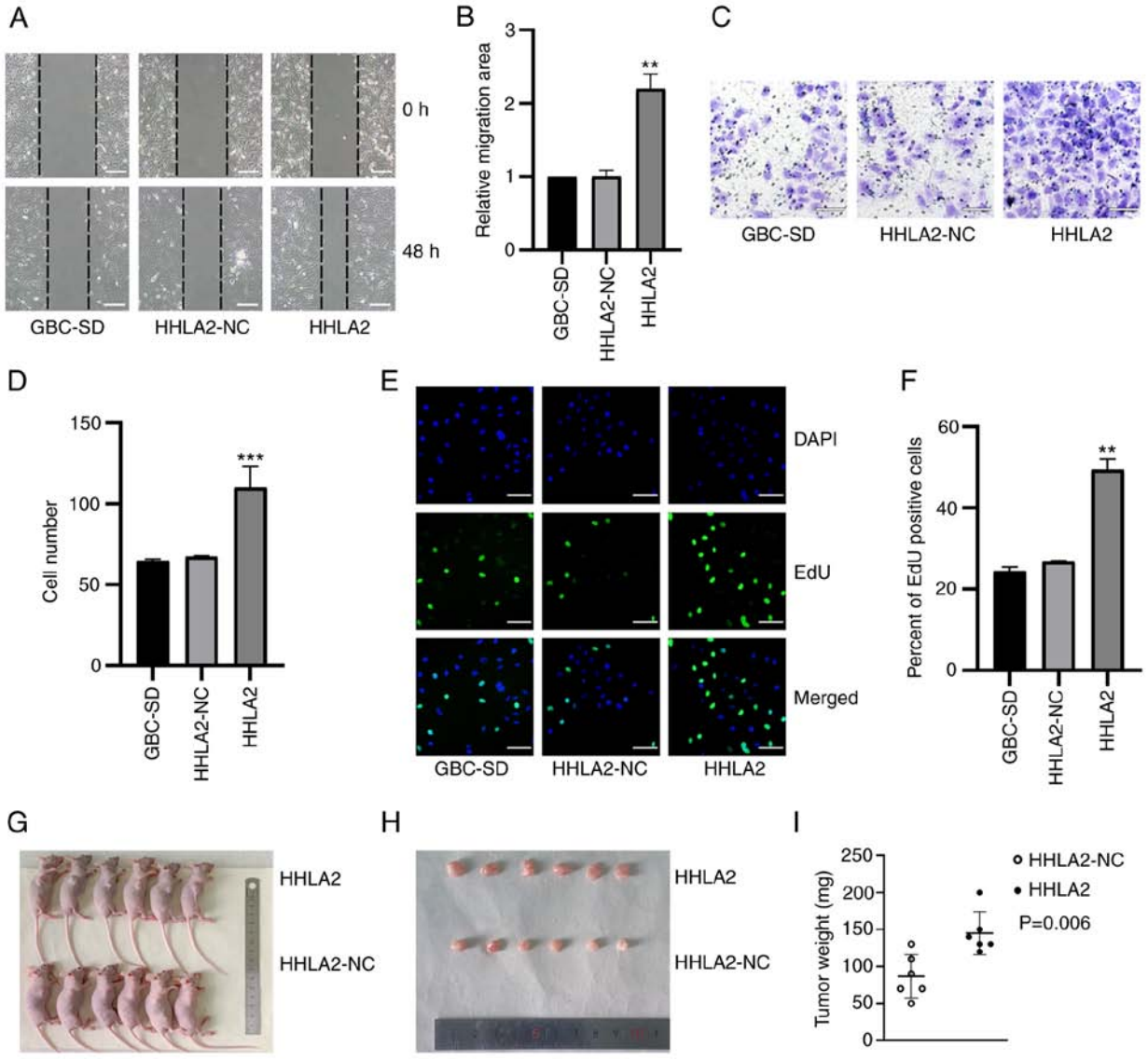

Figure 3. Overexpression of HHLA2 promotes the proliferation, migration and invasion of GBC *in vitro* whilst promoting tumor formation *in vivo*. (A) Wound healing assay and (B) subsequent quantification showed that HHLA2 overexpression enhanced cell migration. Scale bars, 100 μm. (C) HHLA2 overexpression was found to increase invasive capability, (D) which was quantified. Scale bars, 100 μm. (E) The proliferative abilities of the cells overexpressing HHLA2 were higher compared with those of the HLLA2-NC group, (F) according to the quantification. Scale bars, 100 μm. Green, EdU; Blue, DAPI. (G) Representative images of mice in each group harboring the tumors. (H) Overexpression of HHLA2 increases the diameters and the weights of GBC tumors according to the mouse xenograft assay, (I) which was qualified (n=6). **P<0.01 and ***P<0.001 (HHLA2 group vs. HHLA2-NC group). HHLA2, human endogenous retrovirus-H long terminal repeat-associating protein 2; GBC, gall bladder cancer; NC, negative control.

HHLA2 knockdown negatively regulates the tumorigenic ability of GBC cells. The effects of HHLA2 knockdown on GBC-SD migration, invasion and proliferation was subsequently assessed. Results of the wound healing assay revealed that HHLA2-shRNA transfection significantly decreased the migratory ability of GBC-SD cells both alone (Fig. 5A and B) and in the presence of TGF-β1 (Fig. 6A and B). Transwell assay results demonstrated that HHLA2 knockdown in GBC-SD cells significantly inhibited cell invasion (Fig. 5C and D) both alone and in the presence of TGF-β1 (Fig. 6C and D). In addition, results of the EdU assay showed significantly lower proliferation levels in the HHLA2-shRNA group compared with those in the sh-NC group (Fig. 5E and F). In the TGF-β1-treated *in vitro* model, knocking down HHLA2 expression was found to significantly reduce the proliferation of GBC-SD cells (Fig. 6E and F).

GBC-SD stably transfected with HHLA2-shRNA was then used to establish a xenograft model to further investigate its potential role *in vivo*. After 18 days, the tumors in the HHLA2-shRNA group exhibited a significantly light in weight and smaller volume (Fig. 5G-I). These observations suggest that HHLA2 can serve as a therapeutic target for inhibiting the tumorigenicity of GBC.

HHLA2 expression is positively regulated by H19 in GBC. A previous study reported the oncogenic role of H19 in GBC, showing that H19 can promote EMT, migration and invasion in GBC cells (25). After stably transfected with H19 pc-DNA, GBC-SD cells were found with significantly higher expression levels of Col-I, N-cadherin, α-SMA and vimentin but lower expression levels of E-cadherin compared with those in the the H19-NC group (Fig. S2A and B). The H19 overexpression

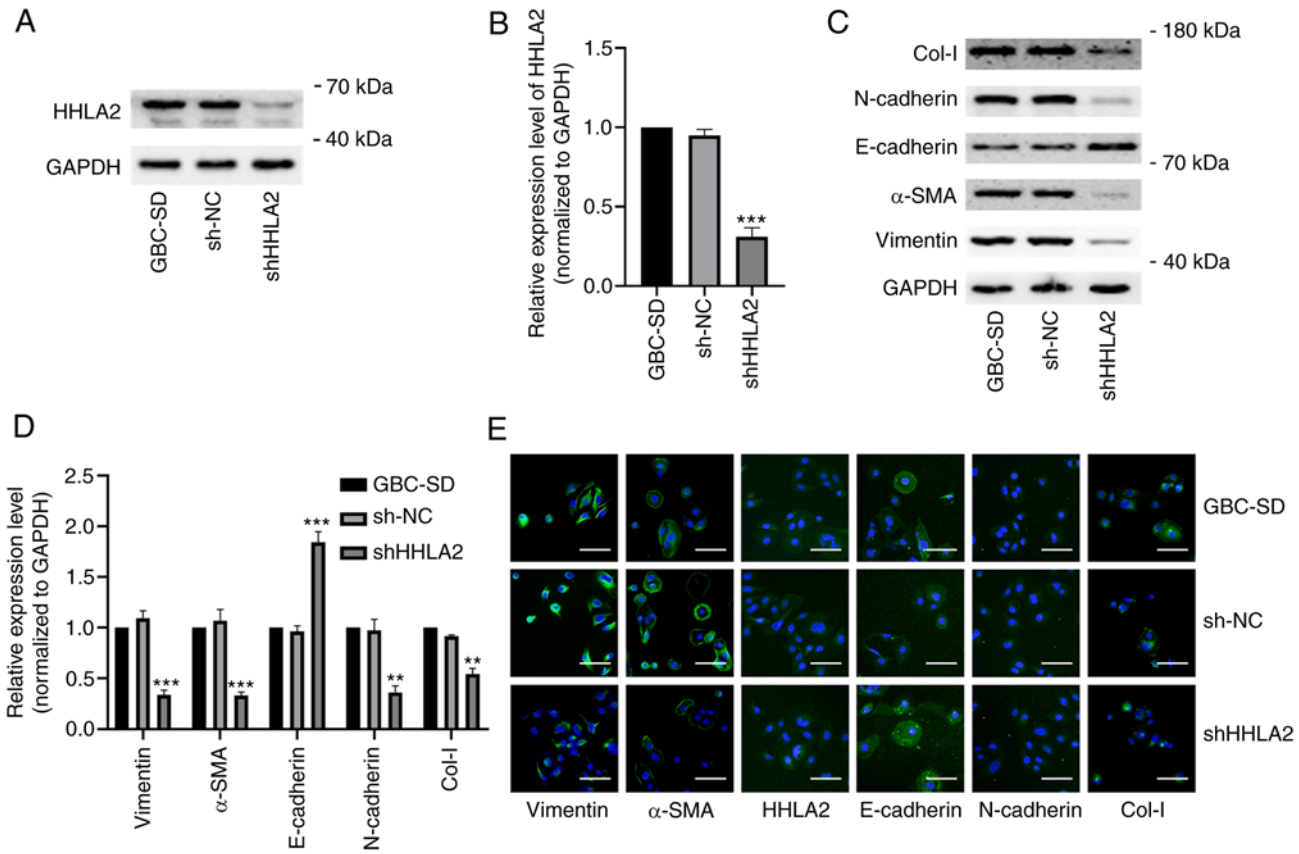

Figure 4. HHLA2 knockdown inhibits the EMT process in GBC cells *in vitro*. (A) HHLA2 expression was significantly decreased after transfection with the HHLA2 shRNA (n=3), (B) according to the quantification. (C) Expression of EMT markers Col-I, N-cadherin, α-SMA and vimentin were decreased whilst that of E-cadherin was increased in GBC cells transfected with the HHLA2 shRNA, (D) according to subsequent quantification. (E) Immunofluorescence staining revealed similar results to western blotting. Scale bars, 100 μm. Green, target protein; Blue, DAPI. **P<0.01 and ***P<0.001 (shHHLA2 group vs. sh-NC group). HHLA2, human endogenous retrovirus-H long terminal repeat-associating protein 2; EMT, epithelial-mesenchymal transition; Col-I, collagen I; α-SMA, α-smooth muscle actin; shRNA or sh, short hairpin RNA; GBC, gall bladder cancer; NC, negative control.

group also showed higher migration and invasion capabilities compared with those in the H19-NC group (Fig. S2C-F). However, the mechanism underlying this require further exploration. Therefore, a GBC cell line stably overexpressing H19 was constructed. The efficiency of H19 overexpression was verified using reverse transcription-quantitative PCR (Fig. 7A). According to the western blotting results, it was found that H19 overexpression significantly increased HHLA2 expression in the GBC-SD cells compared with that in the H19-NC group (Fig. 7B and C).

To explore the possible association between H19 and HHLA2 in EMT, GBC-SD cells stably overexpressing H19 were transiently transfected with HHLA2-shRNA. Both western blotting and immunofluorescence revealed marked downregulation of HHLA2 expression and the expression of EMT markers in the HHLA2 knockdown group, namely that of α-SMA, vimentin, N-cadherin and Col-I (Fig. 7D-F). By contrast, HHLA2 knockdown significantly increased the expression of E-cadherin (Fig. 7D-F). These results suggest that HHLA2 is a key factor in H19-induced GBC-EMT.

H19 promotes GBC migration, invasion and proliferation through HHLA2. Following the observation that HHLA2 is a key factor in H19-induced EMT in GBC-SD, additional assays were performed to investigate the role of HHLA2 in H19 overexpression-induced migration, invasion and proliferation *in vitro*. Results from wound healing assay showed that cells with HHLA2 expression knocked down exhibited significantly lower migratory ability compared with that in the H19 + sh-NC group (Fig. 8A and B). Subsequently, results from the Transwell assay revealed that the invasive ability of cells transfected with HHLA2-shRNA was significantly decreased (Fig. 8C and D). In addition, results of the EdU assay suggested that knockdown of HHLA2 led to a significant reduction of GBC-SD cell proliferation (Fig. 8E and F).

Discussion

The present study aimed to explore the clinical significance of HHLA2 in GBC, one of the most aggressive biliary tract malignancies. In addition, the present study aimed to validate the biological role of HHLA2 in GBC progression, whilst exploring its potential as a novel therapeutic target for GBC treatment. It was first found that in GBC tissues from patients with poorer prognoses and more advanced stage GBC, higher expression of HHLA2 was observed. *In vitro*, overexpression of HHLA2 was found to enhance the aggressive phenotype of GBC. By contrast, knockdown of HHLA2 expression suppressed the progression of GBC both *in vitro* and *in vivo*.

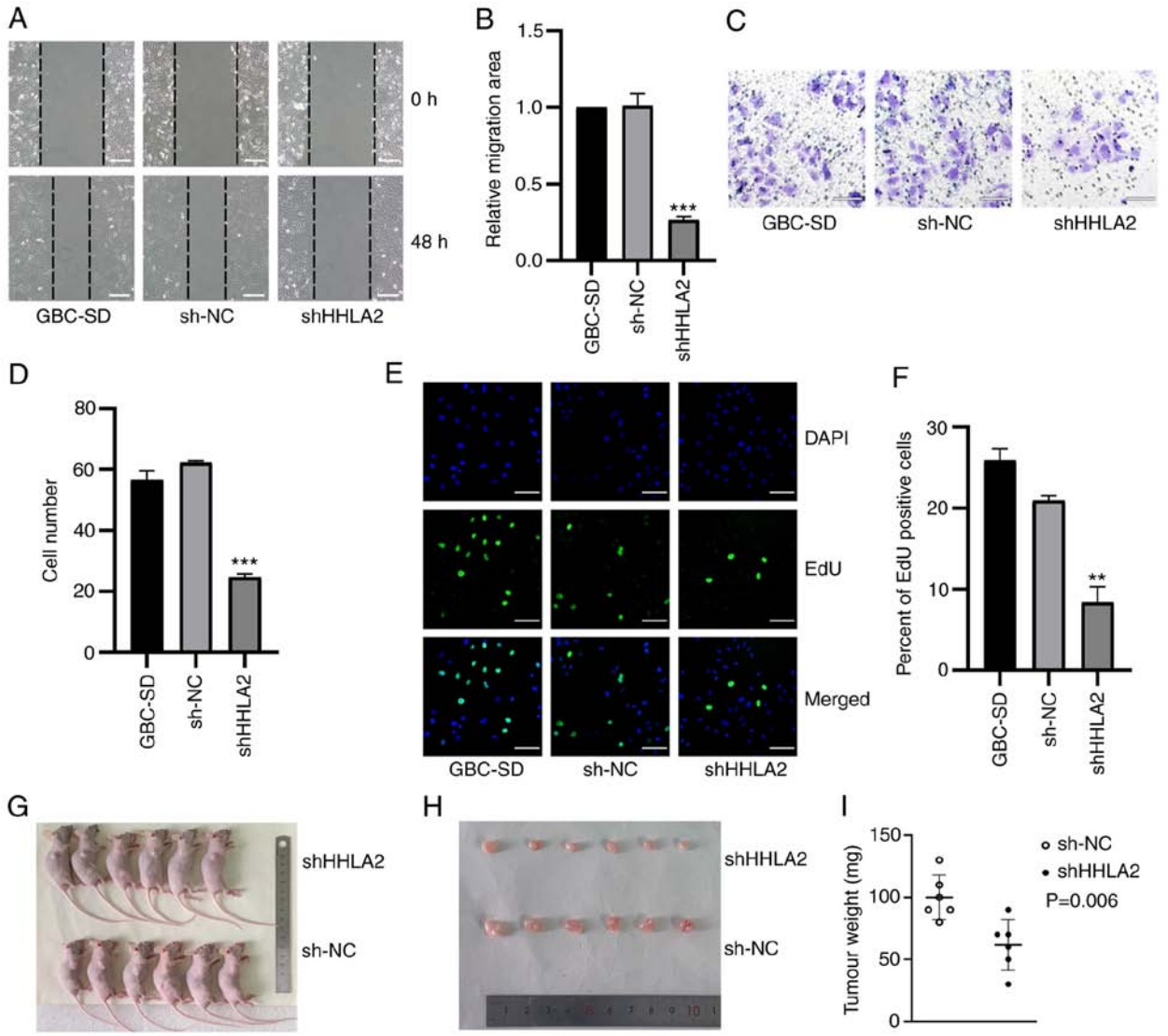

Figure 5. Knocking down HHLA2 expression inhibits the proliferation, migration and invasion of GBC cells *in vitro* and tumour formation *in vivo*. (A) According to the wound-healing assay, which was (B) quantified, HHLA2 knockdown suppressed cell migration. Scale bars, 100 μm. (C) HHLA2 knockdown decreased cell invasion, (D) according to subsequent quantification. Scale bars, 100 μm. (E) Cell proliferation ability in HHLA2 knockdown group was evaluated using EdU assay, which was (F) quantified. Scale bars, 100 μm. Green: EdU; Blue: DAPI. (G) Representative images of mice harboring GBC tumors. HHLA2 knockdown reduced the tumorigenic ability of GBC cells according to the mouse xenograft assay both (H) in terms of size and (I) weight (n=6). **P<0.01 and ***P<0.001 (shHHLA2 group vs. sh-NC group). HHLA2, human endogenous retrovirus-H long terminal repeat-associating protein 2; GBC, gall bladder cancer; shRNA or sh, short hairpin RNA; NC, negative control.

These findings suggest that HHLA2 is a potential therapeutic target for GBC.

In the present study, the relationship between the HHLA2 expression and its biological role in GBC was investigated. It was found that higher expression levels of HHLA2 in patients with GBC were associated with higher Nevin stages, more advanced AJCC stages, more severe tumor invasion and node metastasis, in addition to worse patient OS. The clinical data strongly suggest that HHLA2 can contribute to the progression of GBC. This observation is consistent with that in previous studies, which revealed that HHLA2 can mediate immunosuppressive roles in lung cancer (32), prostate cancer (19) and renal carcinoma (16). However, previous studies also reported ambiguous findings on the role of HHLA2 in tumor progression. In pancreatic, ampullary and ovarian cancers, patients with higher expression of HHLA2 achieved superior prognoses (20,33). These results serve as a reminder that HHLA2 can more than likely mediate different functions depending on the cellular context. To verify the reliability of the clinical results, the function of HHLA2 on GBC was next explored on a cellular level.

To date, 14 protein subtypes in the B7/CD28 family have been discovered (34), the majority which function as immune checkpoint regulators during tumour progression (35-38). However, previous studies have shown that the expression of programmed death-ligand 1 (PD-L1), one of the ligands in the B7 family, is associated with the EMT process and immune evasion in breast cancer, squamous cell carcinoma, non-small-cell lung cancer and cancer stem-like cells (39-42). EMT serves a critical role during early GBC progression (43). Following EMT activation, epithelial cells acquire more mesenchymal properties, resulting in reduced intercellular

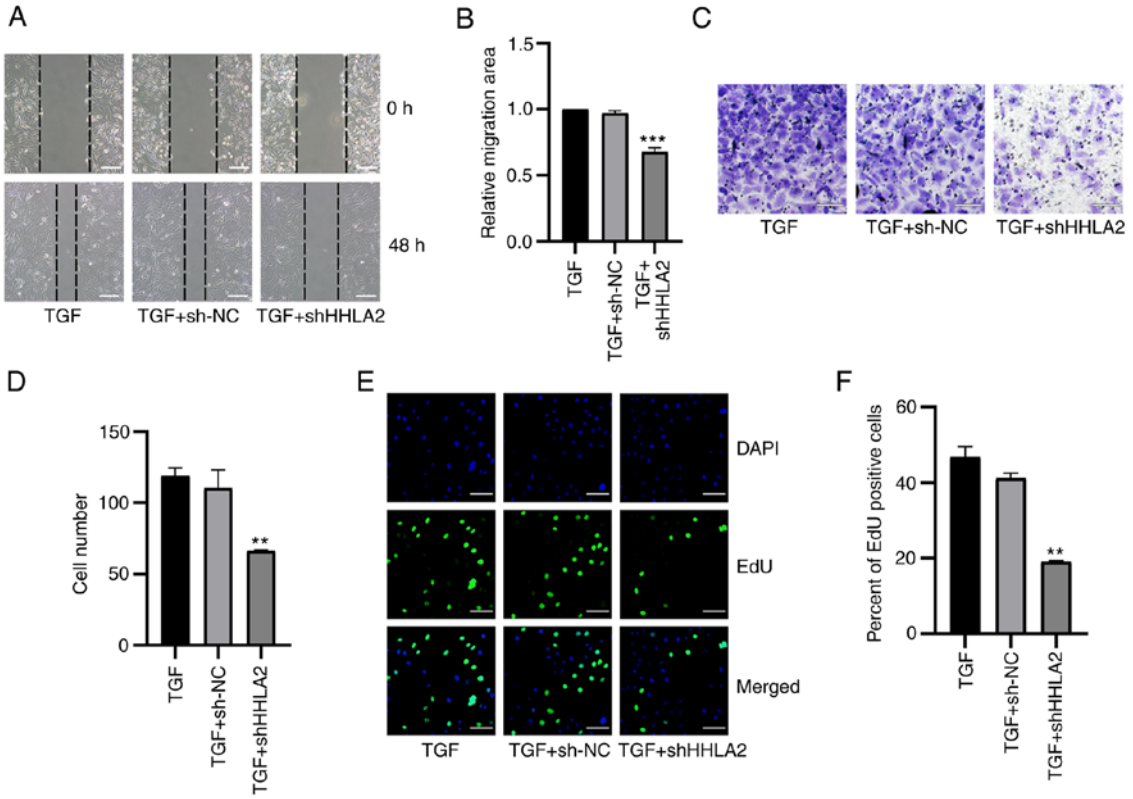

Figure 6. HHLA2 knockdown inhibits TGF-β1-induced proliferation, migration and invasion in the gall bladder cancer cell lines. (A) According to the wound-healing assay, (B) which was quantified, after treatment with TGF-β1 for 48 h, cell migration in the HHLA2 knockdown group was decreased compared with that of the NC group. Scale bar, 100 μm. (C) HHLA2 knockdown downregulated decreased cell invasion, (D) according to subsequent quantification. Scale bars, 100 μm. (E) The proliferative ability of cells after HHLA2 knockdown was decreased compared with that in the TGF + sh-NC group, as determined by EdU assay and (F) was quantified. Scale bars, 100 μm. Green, EdU; Blue, DAPI. **P<0.01 and ***P<0.001 (TGF + shHHLA2 group vs. TGF + sh-NC group). HHLA2, human endogenous retrovirus-H long terminal repeat-associating protein 2; shRNA or sh, short hairpin RNA; NC, negative control.

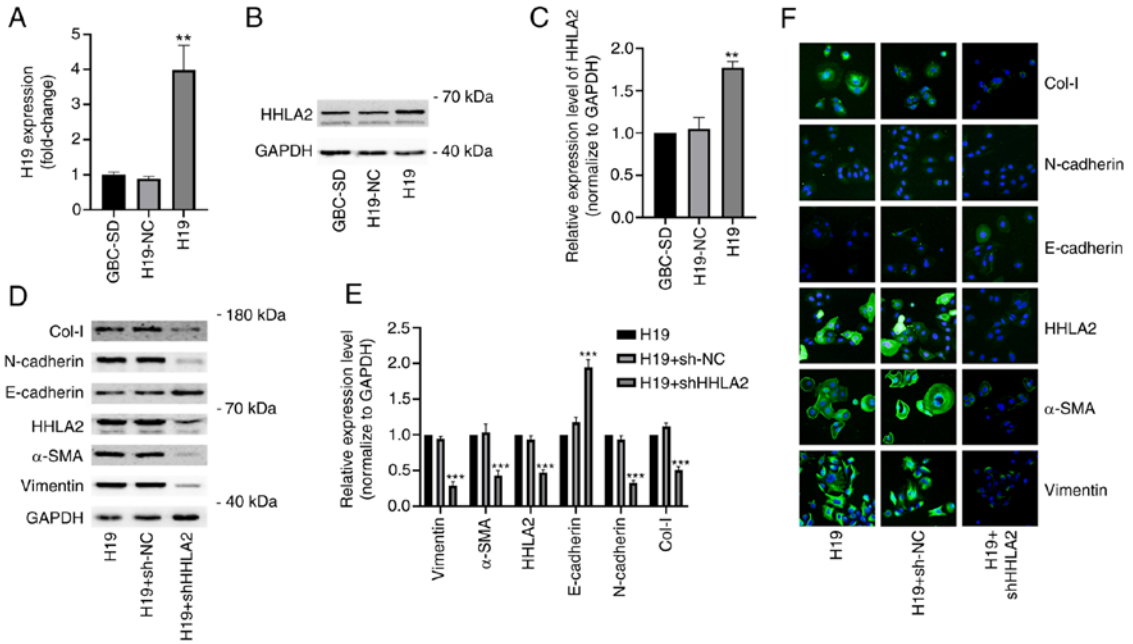

Figure 7. Knockdown of HHLA2 inhibits H19 overexpression-induced EMT in GBC *in vitro*. (A) Reverse transcription-quantitative PCR was used to examine the overexpression efficiency of H19. (B) Western blot analysis showed that H19 overexpression increased HHLA2 expression, (C) according to the quantification. (D) After the knockdown of HHLA2 in GBC cells stably overexpressing H19, the knockdown efficiency of HHLA2 and EMT marker expression were examined using western blotting, (E) which were quantified. Expression of EMT markers Col-I, N-cadherin, α-SMA and vimentin were decreased whilst that of E-cadherin was increased in the HHLA2 knockdown group. (n=3). (F) Similar results were observed according to the immunofluorescence staining images. Scale bars, 100 μm. Green, target protein; Blue, DAPI. **P<0.01 and ***P<0.001 (H19 + shHHLA2 group vs. H19 + sh-NC group). HHLA2, human endogenous retrovirus-H long terminal repeat-associating protein 2; EMT, epithelial-mesenchymal transition; GBC, gall bladder cancer; Col-I, collagen I; α-SMA, α-smooth muscle actin; shRNA or sh, short hairpin RNA; NC, negative control.

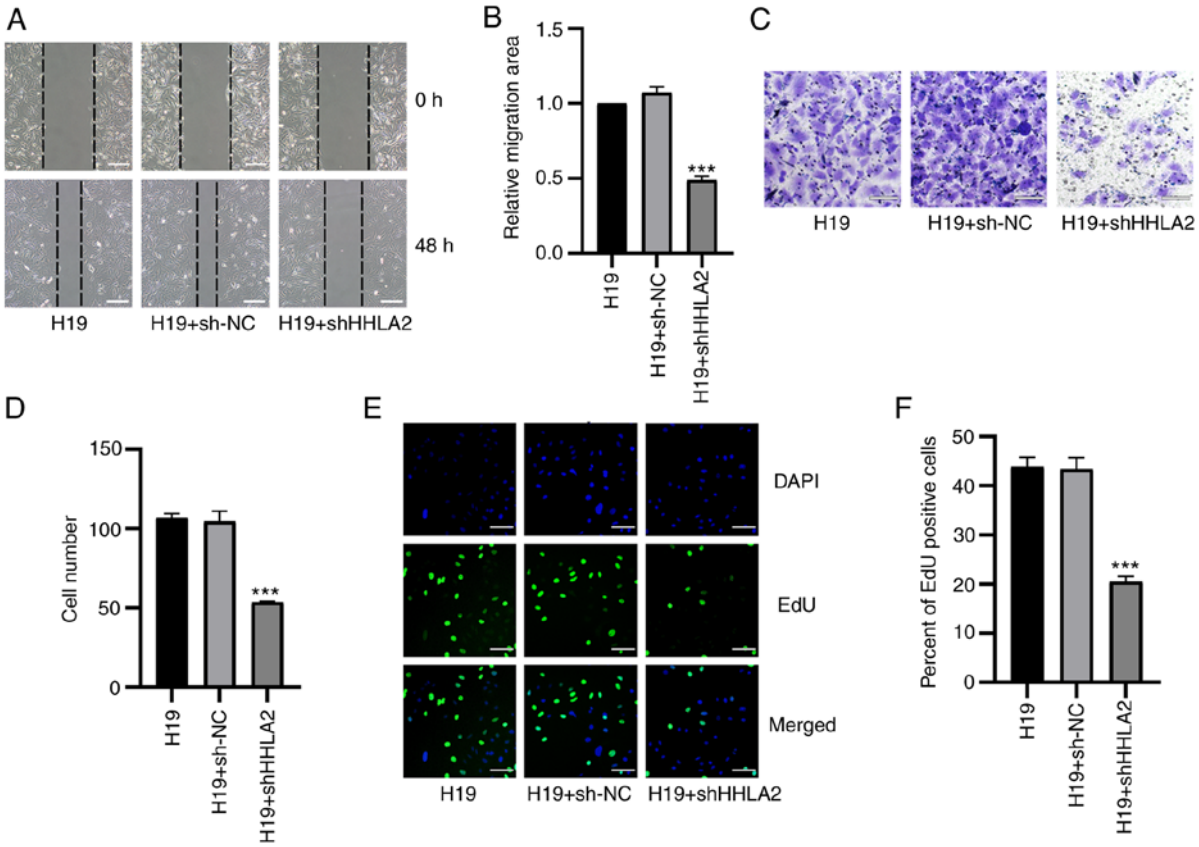

Figure 8. HHLA2 knockdown inhibits H19 overexpression-induced proliferation, migration and invasion in GBC cell lines. (A) From the images of wound healing assay, (B) which were quantified, HHLA2 knockdown reversed H19 overexpression-induced promotion of GBC migration. Scale bars, 100 μm. (C) After transient transfection with HHLA2 shRNA, the H19-overexpressing GBC cell line showed decreased invasive capabilities (D) following quantification. Scale bars, 100 μm. (E) Knocking down HHLA2 expression inhibited the H19 overexpression-induced cell proliferation according to EdU assay, (F) which was quantified. Scale bars, 100 μm. Green, EdU; Blue, DAPI. ***P<0.001 (H19 + shHHLA2 group vs. H19 + sh-NC group). HHLA2, human endogenous retrovirus-H long terminal repeat-associating protein 2; GBC, gall bladder cancer; shRNA or sh, short hairpin RNA; NC, negative control.

adhesion and higher migratory and invasive phenotypes (44). Recently, Cao *et al* (45) reported that PD-L1 can promote EMT and aggressiveness in GBC. Therefore, since it appears to be part of the similar signaling pathway, HHLA2 may also promote GBC progression by directly regulating EMT in GBC cells. Results from the *in vivo* and *in vitro* experiments appeared to support this hypothesis and observations from the clinical data, which showed that overexpression of HHLA2 promoted GBC progression.

Subsequently, by TGF-β1 treatment, an apparently more aggressive GBC-SD cell line (46), was generated, which increased HHLA2 expression. To validate the role of HHLA2 in GBC progression, the GBC cell lines were transfected with the HHLA2 plasmid to overexpress it. Cell proliferation, migration and invasion in GBC cells overexpressing HHLA2 group were all significantly increased, which concurred with the results of the clinical data. Since EMT serves such a key role in the early stages of GBC progression (43), EMT marker expression was next measured. The expression of EMT markers N-cadherin, α-SMA, fibronectin, vimentin and Col-I was all found to be increased, whereas that of E-cadherin was significantly decreased, in the HHLA2-overexpressing GBC-SD cells. *In vivo*, overexpression of HHLA2 resulted in larger tumors being formed. Consistently, investigations into other protein members in the B7 family revealed similar functions in colorectal cancer, pancreatic cancer and hepatocellular cancer (47-49). These EMT mediators confirmed by previous reports will also likely mediate HHLA2-induced EMT in GBC. Kang *et al* (49) previously reported that B7-H3 promoted EMT in hepatocellular carcinoma through the slug pathway, which may also mediate an EMT-promoting role in GBC. Indeed, Lee *et al* (50) previously found that slug was a mediator of EMT in GBC.

To test the therapeutic potential of HHLA2 in GBC, a GBC-SD cell line with HHLA2 expression knocked down was then constructed. Parameters of progression, including proliferation, invasion and migration, were all found to be significantly reduced in the GBC-SD cells after HHLA2 expression was knocked down. This also occurred even in the presence of TGF-β1. In the *in vivo* experiments, HHLA2 knockdown was also observed to reduce GBC tumor size and weight.

In addition to TGF-β1, the present study also investigated another regulatory molecule in HHLA2 expression. Wang *et al* (24,25) previously reported on two occasions that the lncRNA H19 can promote the progression of GBC and its EMT process. Based on these previous observations, the potential regulatory relationship between lncRNA H19 and HHLA2 in GBC was next assessed. In the GBC-SD cell line, overexpression of lncRNA H19 significantly increased HHLA2 expression. In addition, in the rescue experiments,

knockdown of HHLA2 inhibited GBC progression induced by lncRNA H19 overexpression, revealing a regulatory network between H19 and HHLA2 and suggesting the therapeutic potential of HHLA2 in GBC progression. However, it is likely that a complex, as yet unexplored signalling mechanism exist between lncRNA H19 and HHLA2 in the EMT process. Wu *et al* (51) and Yan *et al* (52) previously found that H19 can promote cancer EMT through the Wnt/β-catenin canonical pathway, which was summarized further in a review (51-53). This raises the hypothesis that HHLA2 may be involved in the H19/Wnt/β-catenin axis. Jang *et al* (54) revealed that by recruiting Smad2/3 to the promoter of PD-L1, another member of the B7-family, polo-like kinase 1, enhanced the expression of PD-L1 and promoted EMT in lung adenocarcinoma. This finding also provides further support for the future analysis of the signaling pathways involved in the H19/HHLA2 axis upstream of EMT regulation. In addition to HHLA2, lncRNA H19 may regulate other members of the B7 family upstream of EMT in GBC and other tumors, which require further exploration in the future.

In conclusion, the present study revealed the clinical and biological significance of HHLA2 in GBC. Higher expression levels of HHLA2 were found to associate with worse clinicopathological parameters in patients with GBC and more advanced types of GBC. By contrast, HHLA2 knockdown suppressed GBC progression induced by TGF-β1 and lncRNA H19 overexpression, suggesting that HHLA2 is a potential therapeutic target and prognostic marker for GBC.

Acknowledgements

The authors would like to thank Dr Xingqi Guo (Department of General Surgery, Cancer Hospital of Dalian University of Technology, Shenyang, China) and Dr Huixin Hu (Department of General Surgery, Shengjing Hospital of China Medical University, Shenyang, China) for their assistance in IHC evaluation.

Funding

The present study was supported by the Natural Science Foundation of China (grant no. 81974377 to YT), The Scientific Research Project of Education Department of Liaoning Province (grant no. JC2019017 to YT) and 345 Talent Project of Shengjing Hospital (grant no. 2019-2021 to YT).

Availability of data and materials

The datasets used and/or analyzed during the current study are available from the corresponding author on reasonable request.

Authors' contributions

YT and YZ designed the present study. HL and YZ performed the experiments. CL, YL and FX collected tissue samples and the clinical data. YY, ZL, YS and QL performed the *in vivo* experiments. BW, JZ and CZ analysed and interpreted the data. YL, YS and JZ completed the figures and tables. FX and YT reviewed the manuscript. YT and YZ can authenticate all raw data. All the authors read and approved the final manuscript.

Ethics approval and consent to participate

Ethical approval of animal experiments was approved by the Ethics Committee of Shengjing Hospital of China Medical University (approval no. 2019PS325K; Shenyang, China). All participants consented to an institutional review broad-approved protocol that allows for the comprehensive analysis of tissue samples (Ethics Committee Shengjing Hospital of China Medical University; approval no. 2019PS036K). Informed written consent was obtained from all the participants.

Patient consent for publication

Not applicable.

Competing interests

The authors declare that they have no competing interests.

References

1. Castro FA, Koshiol J, Hsing AW and Devesa SD: Biliary tract cancer incidence in the United States-Demographic and temporal variations by anatomic site. Int J Cancer 133: 1664-1671, 2013.
2. Acharya M, Patkar S, Parray A and Goel M: Management of gallbladder cancer in India. Chin Clin Oncol 8: 35, 2019.
3. Song X, Hu Y, Li Y, Shao R, Liu F and Liu Y: Overview of current targeted therapy in gallbladder cancer. Signal Transduct Targeted Ther 5: 230, 2020.
4. Jin L, Cai Q, Wang S, Wang S, Wang J and Quan Z: Long noncoding RNA PVT1 promoted gallbladder cancer proliferation by epigenetically suppressing miR-18b-5p via DNA methylation. Cell Death Dis 11: 871, 2020.
5. McNamara M, Lopes A, Wasan H, Malka D, Goldstein D, Shannon J, Okusaka T, Knox JJ, Wagner AD, André T, *et al*: Landmark survival analysis and impact of anatomic site of origin in prospective clinical trials of biliary tract cancer. J Hepatol 73: 1109-1117, 2020.
6. Jackson S, Adami H, Andreotti G, Beane-Freeman LE, de González AB, Buring JE, Fraser GE, Freedman ND, Gapstur SM, Gierach G, *et al*: Associations between reproductive factors and biliary tract cancers in women from the biliary tract cancers pooling project. J Hepatol 73: 863-872, 2020.
7. Bray F, Ferlay J, Soerjomataram I, Siegel RL, Torre LA and Jemal A: Global cancer statistics 2018: GLOBOCAN estimates of incidence and mortality worldwide for 36 cancers in 185 countries. CA Cancer J Clin 68: 394-424, 2018.
8. Regmi P, Hu HJ, Chang-Hao Y, Liu F, Ma WJ, Ran CD, Wang JK, Paudyal A, Cheng NS and Li FY: Laparoscopic surgery for oncologic extended resection of T1b and T2 incidental gallbladder carcinoma at a high-volume center: A single-center experience in China. Surg Endos 35: 6505-6512, 2020.
9. Rizzo A, Tavolari S, Ricci AD, Frega G, Palloni A, Relli V, Salati M, Fenocchio E, Massa A, Aglietta M and Brandi G: Molecular features and targeted therapies in extrahepatic cholangiocarcinoma: Promises and failures. Cancers (Basel) 12: 3256, 2020.
10. Valle JW, Kelley RK, Nervi B, Oh DY and Zhu AX: Biliary tract cancer. Lancet 397: 428-444, 2021.
11. Ebata N, Fujita M, Sasagawa S, Maejima K, Okawa Y, Hatanaka Y, Mitsuhashi T, Oosawa-Tatsuguchi A, Tanaka H, Miyano S, *et al*: Molecular classification and tumor microenvironment characterization of gallbladder cancer by comprehensive genomic and transcriptomic analysis. Cancers 13: 733, 2021.
12. Nepal C, Zhu B, O'Rourke C, Bhatt DK, Lee D, Song L, Wang D, Van Dyke AL, Choo-Wosoba H, Liu Z, *et al*: Integrative molecular characterisation of gallbladder cancer reveals micro-environment-associated subtypes. J Hepatol 74: 1132-1144, 2021.
13. Zou W and Chen L: Inhibitory B7-family molecules in the tumour microenvironment. Nat Rev Immunol 8: 467-477, 2008.
14. Zhu Y, Yao S, Iliopoulou BP, Han X, Augustine MM, Xu H, Phennicie RT, Flies SJ, Broadwater M, Ruff W, *et al*: B7-H5 costimulates human T cells via CD28H. Nat Commun 4: 2043, 2013.

15. Crespo J, Vatan L, Maj T, Liu R, Kryczek I and Zou W: Phenotype and tissue distribution of CD28H immune cell subsets. Oncoimmunology 6: e1362529, 2017.
16. Bhatt R, Berjis A, Konge JC, Mahoney KM, Klee AN, Freeman SS, Chen CH, Jegede OA, Catalano PJ, Pignon JC, *et al*: KIR3DL3 is an inhibitory receptor for HHLA2 that mediates an alternative immunoinhibitory pathway to PD1. Cancer Immunol Res 9: 156-169, 2021.
17. Dong Z, Zhang L, Xu W and Zhang G: EGFR may participate in immune evasion through regulation of B7-H5 expression in non-small cell lung carcinoma. Mol Med Rep 18: 3769-3779, 2018.
18. Luo M, Lin Y, Liang R, Li Y and Ge L: Clinical significance of the HHLA2 protein in hepatocellular carcinoma and the tumor microenvironment. J Inflamm Res 14: 4217-4228, 2021.
19. Zhou Q, Li K, Lai Y, Yao K, Wang Q, Zhan X, Peng S, Cai W, Yao W, Zang X, *et al*: B7 score and T cell infiltration stratify immune status in prostate cancer. J Immunother Cancer 9: e002455, 2021.
20. Xu G, Shi Y, Ling X, Wang D, Liu Y, Lu H, Peng Y and Zhang B: HHLA2 predicts better survival and exhibits inhibited proliferation in epithelial ovarian cancer. Cancer Cell Int 21: 252, 2021.
21. Winkle M, El-Daly SM, Fabbri M and Calin GA: Noncoding RNA therapeutics-challenges and potential solutions. Nat Rev Drug Discov 20: 629-651, 2021.
22. Rainier S, Johnson LA, Dobry CJ, Ping AJ, Grundy PE and Feinberg AP: Relaxation of imprinted genes in human cancer. Nature 362: 747-749, 1993.
23. Liu SJ, Dang HX, Lim DA, Feng FY and Maher CA: Long noncoding RNAs in cancer metastasis. Nat Rev Cancer 21: 446-460, 2021.
24. Wang SH, Ma F, Tang ZH, Wu XC, Cai Q, Zhang MD, Weng MZ, Zhou D, Wang JD and Quan ZW: Long non-coding RNA H19 regulates FOXM1 expression by competitively binding endogenous miR-342-3p in gallbladder cancer. J Exp Clin Cancer Res 35: 160, 2016.
25. Wang SH, Wu XC, Zhang MD, Weng MZ, Zhou D and Quan ZW: Upregulation of H19 indicates a poor prognosis in gallbladder carcinoma and promotes epithelial-mesenchymal transition. Am J Cancer Res 6: 15-26, 2016.
26. Giannis D, Cerullo M, Moris D, Shah KN, Herbert G, Zani S, Blazer DG III, Allen PJ and Lidsky ME: Validation of the 8th edition American joint commission on cancer (AJCC) gallbladder cancer staging system: Prognostic discrimination and identification of key predictive factors. Cancers 13: 547, 2021.
27. Nagtegaal ID, Odze RD, Klimstra D, Paradis V, Rugge M, Schirmacher P, Washington KM, Carneiro F and Cree IA; WHO Classification of Tumours Editorial Board: The 2019 WHO classification of tumours of the digestive system. Histopathology 76: 182-188, 2020.
28. Xu X, He M, Wang H, Zhan M and Yang L: Development and validation of a prognostic nomogram for gallbladder cancer patients after surgery. BMC Gastroenterol 22: 200, 2022.
29. Camp RL, Dolled-Filhart M and Rimm DL: X-tile: A new bio-informatics tool for biomarker assessment and outcome-based cut-point optimization. Clin Cancer Res 10: 7252-7259, 2004.
30. Livak KJ and Schmittgen TD: Analysis of relative gene expression data using real-time quantitative PCR and the 2(-Delta Delta C(T)) method. Methods 25: 402-408, 2001.
31. Clark JM and Sun D: Guidelines for the ethical review of laboratory animal welfare People's Republic of China National Standard GB/T 35892-2018 [Issued 6 February 2018 Effective from 1 September 2018]. Animal Models Exp Med 3: 103-113, 2020.
32. Cheng H, Janakiram M, Borczuk A, Lin J, Qiu W, Liu H, Chinai JM, Halmos B, Perez-Soler R and Zang X: HHLA2, a new immune checkpoint member of the B7 family, is widely expressed in human lung cancer and associated with EGFR mutational status. Clin Cancer Res 23: 825-832, 2017.
33. Boor P, Sideras K, Biermann K, Aziz MH, Levink IJM, Mancham S, Erler NS, Tang X, van Eijck CH, Bruno MJ, *et al*: HHLA2 is expressed in pancreatic and ampullary cancers and increased expression is associated with better post-surgical prognosis. Br J Cancer 122: 1211-1218, 2020.
34. Zhong C, Lang Q, Yu J, Wu S, Xu F and Tian Y: Phenotypical and potential functional characteristics of different immune cells expressing CD28H/B7-H5 and their relationship with cancer prognosis. Clin Exp Immunol 200: 12-21, 2020.
35. Seaman S, Zhu Z, Saha S, Zhang XM, Yang MY, Hilton MB, Morris K, Szot C, Morris H, Swing DA, *et al*: Eradication of tumors through simultaneous ablation of CD276/B7-H3-positive tumor cells and tumor vasculature. Cancer Cell 31: 501-515.e8, 2017.
36. Schildberg FA, Klein SR, Freeman GJ and Sharpe AH: Coinhibitory pathways in the B7-CD28 ligand-receptor family. Immunity 44: 955-972, 2016.
37. Marangoni F, Zhakyp A, Corsini M, Geels SN, Carrizosa E, Thelen M, Mani V, Prüßmann JN, Warner RD, Ozga AJ, *et al*: Expansion of tumor-associated Treg cells upon disruption of a CTLA-4-dependent feedback loop. Cell 184: 3998-4015.e19, 2021.
38. Nishimura CD, Pulanco MC, Cui W, Lu L and Zang X: PD-L1 and B7-1 cis-interaction: New mechanisms in immune checkpoints and immunotherapies. Trends Mol Med 27: 207-219, 2021.
39. Chen L, Gibbons DL, Goswami S, Cortez MA, Ahn YH, Byers LA, Zhang X, Yi X, Dwyer D, Lin W, *et al*: Metastasis is regulated via microRNA-200/ZEB1 axis control of tumour cell PD-L1 expression and intratumoral immunosuppression. Nat Commun 5: 5241, 2014.
40. Lee Y, Shin J, Longmire M, Wang H, Kohrt HE, Chang HY and Sunwoo JB: CD44+ cells in head and neck squamous cell carcinoma suppress T-cell-mediated immunity by selective constitutive and inducible expression of PD-L1. Clin Cancer Res 22: 3571-3581, 2016.
41. Alsuliman A, Colak D, Al-Harazi O, Fitwi H, Tulbah A, Al-Tweigeri T, Al-Alwan M and Ghebeh H: Bidirectional crosstalk between PD-L1 expression and epithelial to mesenchymal transition: significance in claudin-low breast cancer cells. Mol Cancer 14: 149, 2015.
42. Hsu JM, Xia W, Hsu YH, Chan L, Yu WH, Cha JH, Chen CT, Liao HW, Kuo CW, Khoo KH, *et al*: STT3-dependent PD-L1 accumulation on cancer stem cells promotes immune evasion. Nat Commun 9: 1908, 2018.
43. Xu S, Zhan M and Wang J: Epithelial-to-mesenchymal transition in gallbladder cancer: From clinical evidence to cellular regulatory networks. Cell Death Discov 3: 17069, 2017.
44. Krebs AM, Mitschke J, Losada MA, Schmalhofer O, Boerries M, Busch H, Boettcher M, Mougiakakos D, Reichardt W, Bronsert P, *et al*: The EMT-activator Zeb1 is a key factor for cell plasticity and promotes metastasis in pancreatic cancer. Nat Cell Biol 19: 518-529, 2017.
45. Cao L, Bridle KR, Shrestha R, Prithviraj P, Crawford DHG and Jayachandran A: CD73 and PD-L1 as potential therapeutic targets in gallbladder cancer. Int J Mol Sci 23: 1565, 2022.
46. Shi Y, Sun L, Zhang R, Hu Y, Wu Y, Dong X, Dong D, Chen C, Geng Z, Li E and Fan Y: Thrombospondin 4/integrin α2/HSF1 axis promotes proliferation and cancer stem-like traits of gallbladder cancer by enhancing reciprocal crosstalk between cancer-associated fibroblasts and tumor cells. J Exp Clin Cancer Res 40: 14, 2021.
47. Yin Y, Shi L, Yang J, Wang H, Yang H and Wang Q: B7 family member H4 induces epithelial-mesenchymal transition and promotes the proliferation, migration and invasion of colorectal cancer cells. Bioengineered 13: 107-118, 2022.
48. Kang JH, Jung MY and Leof EB: B7-1 drives TGF-β stimulated pancreatic carcinoma cell migration and expression of EMT target genes. PLoS One 14: e0222083, 2019.
49. Kang F-B, Wang L, Jia H-C, Li D, Li H-J, Zhang Y-G and Sun D-X: B7-H3 promotes aggression and invasion of hepatocellular carcinoma by targeting epithelial-to-mesenchymal transition via JAK2/STAT3/Slug signaling pathway. Cancer Cell Int 15: 45, 2015.
50. Lee DW, Lee SH, Kim JS, Park J, Cho YL, Kim KS, Jo DY, Song IC, Kim N, Yun HJ, *et al*: Loss of NDRG2 promotes epithelial-mesenchymal transition of gallbladder carcinoma cells through MMP-19-mediated Slug expression. J Hepatol 63: 1429-1439, 2015.
51. Wu K, Liang W, Feng L, Pang JX, Waye MMY, Zhang JF and Fu WM: H19 mediates methotrexate resistance in colorectal cancer through activating Wnt/β-catenin pathway. Exp Cell Res 350: 312-317, 2017.
52. Yan L, Yang S, Yue CX, Wei XY, Peng W, Dong ZY, Xu HN, Chen SL, Wang WR, Chen CJ and Yang QL: Long noncoding RNA H19 acts as a miR-340-3p sponge to promote epithelial-mesenchymal transition by regulating YWHAZ expression in paclitaxel-resistant breast cancer cells. Environ Toxicol 35: 1015-1028, 2020.
53. Wu B, Zhang Y, Yu Y, Zhong C, Lang Q, Liang Z, Lv C, Xu F and Tian Y: ViaLong noncoding RNA H19: A novel therapeutic target emerging in oncology regulating oncogenic signaling pathways. Front Cell Dev Biol 9: 796740, 2021.
54. Jang H-R, Shin S-B, Kim C-H, Won J-Y, Xu R, Kim D-E and Yim H: PLK1/vimentin signaling facilitates immune escape by recruiting Smad2/3 to PD-L1 promoter in metastatic lung adenocarcinoma. Cell Death Diff 28: 2745-2764, 2021.